CURCUMIN DELIVERY SYSTEMS AS DRESSING COMPONENTS FOR THE TREATMENT OF DIABETIC FOOT ULCERS: TESTS ON MACROPHAGES POLARIZATION

Karolina Wójcik[1]*, Anna Kusibab[1], Ana Beatriz Sousa[2,3,4], Judite Novais Barbosa[2,3,4], Elżbieta Pamuła[1]

[1] AGH University of Krakow,
Faculty of Materials Science and Ceramics,
Department of Biomaterials and Composites,
al. A. Mickiewicza 30, 30-059 Krakow, Poland
[2] i3S – Instituto de Investigação e Inovação em Saúde,
Universidade do Porto, Rua Alfredo Allen 208,
4200-135 Porto, Portugal
[3] INEB – Instituto de Engenharia Biomédica,
Universidade do Porto, Rua Alfredo Allen 208,
4200-135 Porto, Portugal
[4] Instituto Ciências Biomédicas Abel Salazar
da Universidade do Porto, Rua de Jorge Viterbo
Ferreira 228, 4050-313 Porto, Portugal
*e-mail: karolina.wojcik1@interia.pl

Abstract

The natural wound healing process consists of four basic phases: homeostasis, inflammation, proliferation, and remodelling. Macrophages play an important role in the body's response to biomaterials, as they are modulators of the wound healing process and can polarize into different phenotypes capable of inducing both deleterious and beneficial effects on tissue repair. Curcumin (CU) is known for its anti-inflammatory properties and has the potential to treat diabetic foot ulcers, but it should be delivered to wounds in a controlled manner. In this study, the encapsulation of curcumin in polymeric microparticles based on poly(sebacic anhydride) (PSA) was developed using an emulsification method. PSA-based microparticles containing different concentrations of CU were obtained: 0% weight (wt). CU (unloaded microparticles), 5, 10, and 20 wt% CU. CU encapsulation efficiency and loading were determined using a fluorescence-based calibration curve method and semi-quantitative Fourier-transform infrared spectroscopy (FTIR) analysis. The potential cytotoxicity of the obtained biomaterials in contact with primary human macrophages and their susceptibility to polarization from the M1 (pro-inflammatory) phenotype to the M2 (anti-inflammatory) phenotype were evaluated. The morphology of cells cultured in contact with polymeric microparticles was evaluated using phalloidin red and 4',6-diamidino-2-phenylindole (DAPI) staining. Macrophage phenotype was assessed using flow cytometry. The obtained biomaterials showed no cytotoxic effect on primary human macrophages. Flow cytometry studies showed enhanced polarization of macrophages into anti-inflammatory M2 phenotype when exposed to microparticles loaded with CU and CU powder as compared to unloaded microparticles.

Keywords: *curcumin, immunomodulation, inflammation, macrophage polarization, polymeric microparticles, wound healing*

[Engineering of Biomaterials 168 (2023) 15-24]

doi:10.34821/eng.biomat.168.2023.15-24

Submitted: 2023-04-25, Accepted: 2023-05-12, Published: 2023-05-18

Introduction

Diabetes mellitus is a chronic disease characterized by hyperglycemia that can lead to various complications, such as diabetic wounds and ulcers. These complications require long-term treatment and negatively affect the patient's quality of life [1]. High and persistent glucose levels can cause vascular damage, which can affect and harm nerves, leading to neuropathy that may cause severe damage, resulting in serious infections and ulcers [2].

According to epidemiological studies by the International Diabetes Federation (IDF), around 463 million people suffered from diabetes in 2019, and this number is estimated to increase to 578 million in 2030 and 700 million in 2045, with 20% of the patients developing diabetic wounds [3]. Another study showed that 3.1-11.8% of patients with diabetes have foot ulcers and are 10-20 times more likely to suffer a lower limb amputation [4]. In addition, diabetic foot ulcers are known to affect patients economically, as their healthcare costs are 5 times higher than those of diabetic patients without foot ulcers [5]. Diabetes complicates and prolongs the natural wound-healing process, as it stops it in the inflammatory phase [6]. Impaired function and decreased neutrophil infiltration lead to oxidative stress and the release of pro-inflammatory cytokines. Prolonged exposure to reactive oxygen species (ROS) causes cellular dysfunction and destructive oxidation of intracellular lipids, nucleic acids, and proteins. Peroxisome proliferator-activated receptor (PPARγ) expression is dysregulated in normal wound healing facilitating the transition of macrophages from an M1 (pro-inflammatory) to an M2 (anti-inflammatory) like phenotype, critical for normal wound healing [7].

Macrophages are key modulators of the wound healing process as they play a unique role in ensuring proper healing. Initially, pro-inflammatory macrophages (M1) infiltrate after injury to clear the wound of bacteria, foreign debris, and dead cells. In acute wounds, as the tissue begins to repair, the overall macrophage population transitions to the M2 phenotype that promotes anti-inflammatory effects and the migration and proliferation of fibroblasts, keratinocytes, and endothelial cells to restore the dermis, epidermis, and vasculature [8]. Moreover, macrophages express growth factors and cytokines essential for angiogenesis, cell proliferation, and extracellular matrix deposition [9]. Eventually, the wound closes and a scar forms. Early in the final phase of the remodeling phase, macrophages release matrix metalloproteinases (MMPs) to degrade the provisional extracellular matrix, and then apoptose so that the skin can mature to its original intact state [8]. The macrophage phenotype gradually changes throughout the healing process from an initial pro-inflammatory M1 phenotype characteristic of the acute response to a pro-regenerative M2 phenotype that allows accurate tissue repair [9]. In chronic wounds, pro-inflammatory macrophages persist without transitioning to anti-inflammatory phenotypes; which is thought to contribute to the impairment in tissue repair [8].

Nanotechnology-based therapies have emerged as a promising treatment for chronic diabetic foot ulcers, due to their unique properties and specific functional properties [1]. It has been shown that curcumin (CU) as an active substance possesses significant anti-inflammatory, anti-oxidant, anti-carcinogenic, anti-mutagenic, anticoagulant, and anti-infective properties [7]. CU promotes healing by acting on various stages of the natural wound healing process. It can enhance granulation, tissue formation, collagen deposition, tissue remodelling, and wound contraction [7].

The aim of this study was to develop curcumin delivery systems made of degradable polymer microparticles and to assess their anti-inflammatory properties in contact with human macrophages.

Materials and Methods

Manufacturing of microparticles

Polymeric microparticles were manufactured using a single oil-in-water (O/W) emulsification with the solvent evaporation method. The water phase (W) was a 2% poly(vinyl alcohol) solution (PVA, Mw = 31 kDa, Sigma-Aldrich, Mowiol 4-88, CAS: 9002-89-5) while the oil phase (O) consisted of poly(sebacic anhydride) (PSA, Silesian University of Technology [10]) dissolved in dichloromethane (DCM, 99.8% pure P.A., POCH S.A, CAS: 75-09-2) (2% w/v) with CU (Sigma-Aldrich, C7727-500MG, CAS:458-37-7) as an active substance. The chemical formulas of CU and PSA are shown in FIG. 1 and 2, respectively.

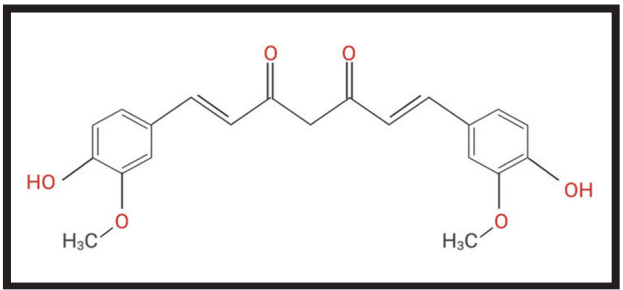

FIG. 1. Molecular structure of curcumin.

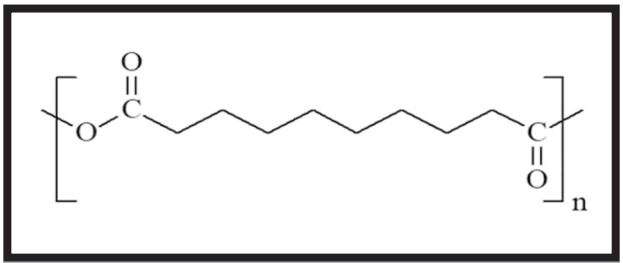

FIG. 2. Poly(sebacic anhydride) structural formula.

Polymeric microparticles that contained different weight concentrations of CU were prepared according to a method described earlier [11]: PSA/DCM – unloaded sample and PSA/DCM+CU with different concentrations of CU: 5, 10, and 20 wt% CU.

The calculated masses of curcumin required to prepare samples with CU concentrations: 0, 5, 10, and 20 wt%, were respectively weighted. Then, a 2% w/v PSA solution in DCM was prepared as an oil phase. 3 mL of the oil phase was homogenized for 90 s, at an amplitude of 40%, and slowly dripped into the water phase (20 mL). Subsequently, beakers placed in crystallizers with ice (to cool the PVA solution) were then placed on a magnetic stirrer to mix their contents. The mixing process was carried out for 5 h (until the solvent evaporated), at a set stirring speed of 1200 rpm at room temperature. The resulting emulsions were then centrifuged using a centrifuge (3-30 K, Sigma). Centrifugation parameters were: v = 15,000 rpm, t = 20 min, T = 4°C. Next, UHQ water was added and the samples were centrifuged 3 times. Supernatants (1.5 mL for each sample) were collected to assess encapsulation efficiency (EE). 10 µL of the suspension was placed on a microscope slide and 3 images per sample were taken for further characterization of the manufactured microparticles. The remaining microparticles were frozen at -80ºC for 24 h. Microparticles were freeze-dried for 48 h.

The diameters of the manufactured polymeric microparticles were measured using ImageJ software. Histograms of the size distribution were prepared based on the obtained results using Python software.

Manufacturing efficiency (ME) was calculated using the formula (1):

$$ME = \frac{\text{mass of sample after liophylization}}{\text{mass of PSA in sample+mass of CU in sample}} \cdot 100\% \quad (1)$$

Characterization of microparticles

The encapsulation efficiency of CU was determined in the supernatants after the centrifugation process using a fluorometric assay. The supernatant samples were treated with DMSO (POCH S.A.) at a volume ratio of 1:10 to dilute the residual CU. CU in known concentrations (0-100 µg/mL, step 10 µg/mL) was dissolved in the same mixture of water: DMSO (1:10) for the preparation of the calibration curve. The linear relationship was estimated in the range of 0-20 µg/mL CU. Samples of both calibrators and supernatants diluted in DMSO were placed in a black 96-well TCPS plate (100 µL/well, n = 3 for each sample). Excitation wavelengths of 485-412 nm and emission wavelengths of 590–510 nm were used in a plate reader (FluoStar OMEGA, BMG LabTech) [11].

The encapsulation efficiency (EE) was determined as (2):

$$EE = \frac{\text{encapsulated CU}}{\text{initial CU addition}} \cdot 100\% \quad (2)$$

and drug loading (DL) was calculated as follows (3):

$$DL = \frac{\text{encapsulated CU}}{\text{MP mass}} \cdot 100\% \quad (3)$$

FTIR analysis was performed using PerkinElmer FT-IR spectrometer to identify characteristic chemical groups and bonds present in the curcumin molecule, and to determine the encapsulation efficiency, a semi-quantification approach was used. The analysis was carried out at room temperature (21°C) and low humidity (approx. 68%). FTIR spectra were analyzed using PerkinElmer Spectrum IR software.

Primary human monocyte isolation and macrophage differentiation

Human monocytes were isolated from the peripheral blood of healthy blood donors by negative selection, using methods described in [12]. Briefly, buffy coats were centrifuged at room temperature for 20 min at 1200 g (Eppendorf Centrifuge 5810R, VWR International LLC, Radnor, PA, USA), with acceleration set at 5 and brake set to 0, for blood components separation. Peripheral blood mononuclear cells (PBMC) were collected and incubated with RosetteSep™ Human Monocyte Enrichment Cocktail (67 µL per 1 mL of RBC-PBMC, StemCell Technologies™, Vancouver, Canada) at room temperature for 20 min under slow orbital agitation. The mixture was diluted at a 1:1 ratio with 2% heat in-activated FBS (Biowest, Riverside, MO, USA) in PBS, gently layered over Histopaque-1077 (Sigma-Aldrich Co., St Louis, MO, USA) and centrifuged as former.

The enriched monocyte layer was collected and washed three times with PBS by centrifugation at 7 min, 1300 rpm, at room temperature (Eppendorf Centrifuge 5810R, VWR International LLC, Radnor, PA, USA) [13].

For macrophage differentiation, $0.5x10^6$ cells/mL were seeded on glass coverslips in 24-well plates, and cultured for 7 days in complete RPMI media, supplemented with 10% FBS, in the presence of 50 ng/mL of rh M-CSF (ImmunoTools, Friesoythe, Germany). After 7 days of differentiation, the cell culture media was changed, and M-CSF was removed [12,13].

To polarize macrophages towards M1 phenotype (pro-inflammatory), on day 7 of culture, media was replaced, and monocytes/macrophages were stimulated with 10 ng/mL lipopolysaccharide (LPS, *Escherichia coli* serotype O55:B5, Sigma-Aldrich Co., St Louis, MO, USA) and 50 ng/mL recombinant interferon-gamma (rhIFN-γ, ImmunoTools, Friesoythe, Germany) [12].

The manufactured PSA-based microparticles were added to the activated cells on day 8 to investigate their anti-inflammatory properties, interpreted as the ability of the cells to shift their phenotype from M1 (pro-inflammatory) towards M2 (anti-inflammatory).

Evaluation of the cells morphology was performed by fluorescent staining with phalloidin red and DAPI. Briefly, cells were fixed with 4% paraformaldehyde solution (PFA: 50-00-0; Sigma-Aldrich®) for 20 min and afterward washed with PBS (3x5 min, under agitation). The aldehydes were blocked with ammonium chloride (NH_4Cl, 213330, Sigma-Aldrich®, 50 mM) for 10 min. Cells were washed with PBS (3x5 min). The membrane was permeabilized with 0.2% Triton X-100: 648466 (VWR International, Material de Laboratório, Lda) for 5 min. Cells were washed with PBS (3x5 min, under agitation), blocked with 1% bovine serum albumin (BSA: A4919, Sigma-Aldrich®), for 1 h, followed by an incubation with phalloidin red (1:200, Alexa FluorTM 594 phalloidin: A12381, ThermoFisher Scientific, Invitrogen) for 20 min. Cells were washed with PBS (3x5 min, under agitation). Nuclei were stained with DAPI (1:1000, D3571; Alfagene) for 5 min. PBS washing was repeated (3x5 min, under agitation). All steps were performed at room temperature (RT, 21ºC). Images were taken under a motorized inverted epifluorescence microscope (Leica DMI6000 FFW, Leica Microsystems, Germany).

LDH assay (Promega) was performed to assess the cytotoxicity of the developed particles. The assay was conducted on the following types of samples: CU, unloaded microparticles (PSA-based), and microparticle samples with CU at the concentrations of 0.77 mg/mL, and 1.54 mg/mL. Briefly, a 50 µL medium of each sample was placed in the wells of a 96-well plate. Next, 50 µL of CytoTox96® Assay (Promega, Madison, WI, USA), was added to bind with LDH, and the plate was left to incubate for 30 min (protected from light). Next, 50 µL of stop solution was added to block the reaction. A blank control (only a culture medium) and a positive control were also included. Cytotoxicity was defined as the percentage of LDH activity in culture media, relative to LDH activity of the positive control [13]. The presence of LDH was measured in cell-free culture supernatants. The total LDH release was determined using LDH positive control provided by the CytoTox96® assay. Three replicates for each measurement were included for each condition. The average of the three measurements was determined.

24 hours after incubation of macrophages with microparticles, macrophage polarization was evaluated by flow cytometry. Macrophages were identified using the following surface markers: CD14 (as a pan macrophage marker), CD86 (M1 phenotype), and CD163 (M2 phenotype). 2 µL for CD14 and CD86 marker, and 5 µL for CD163 marker was added to the corresponding well.

The following samples were analyzed: control sample (primary human macrophages), CU powder, unloaded microparticles (PSA-based matrix, MPs), and polymeric microparticles loaded with curcumin at a concentration of 0.77 mg/mL (MPs_CU_0.77) and 1.54 mg/mL (MPs_CU_1.54).

The macrophages were washed, resuspended in FACS buffer (PBS, 2% FBS, 0.01% sodium azide) (Sigma-Aldrich Co., St Louis, MO, USA) and incubated with the following antibodies: anti-human CD14-APC (clone MEM-18), CD86-FITC (clone BU63) (all from ImmunoTools, Friesoythe, Germany) and CD163-PE (clone GHI/61) (BD Biosciences, San Jose, CA, USA) for 30 min at RT. Isotype-matched antibodies were used as negative controls, to define background staining [12].

After additional washing, 10,000 cells, gated according to forward and side scatter parameters, were acquired using a BD FACSCanto IITM flow cytometer (Becton Dickinson) using FACSDivaTM software (both from BD Biosciences, San Jose, CA, USA). Data were analyzed using FlowJo software (BD Biosciences, San Jose, CA, USA, version 10), and the percentage of CD14, CD86, and CD163 positive cells was calculated by subtracting the corresponding isotype control [12].

Results and Discussion

Properties of microparticles

The preparation method of microparticles was emulsification with solvent evaporation. The following sample types were analyzed: pure CU powder, unloaded PSA microparticles, and curcumin-loaded microparticles with concentrations of 5, 10, and 20% by weight of CU. The highest manufacturing efficiency was obtained for a polymeric sample with a concentration of 10 wt% CU, and it was equal to 74%. The manufactured PSA-based microparticles were spherical with a median diameter from 5.2 to 8.4 µm (FIG. 3A-H). The CU-loaded microparticles were yellow (FIG. 4B-D) and because of the fact that CU is fluorescent, the microparticles glowed intensely green under the fluorescence microscope, and exhibited fluorescent properties (FIG. 4B-D). It indicated that CU was effectively and uniformly encapsulated within the PSA microparticles (only black background was visible in CU-free sample image, FIG. 4A). The fluorescence of curcumin allowed the encapsulation and loading efficiency to be tested with a fluorescence reader, so the fluorescence images obtained (FIG. 4) not only prove the presence of curcumin in the particles, but also confirm the fact that it is fluorescent and explain the basis for the choice of this particular research method.

Encapsulation efficiency and loading efficiency

Encapsulation efficiency (EE) of CU in microparticles was calculated using a calibration curve, separately for supernatants and particles alone (TABLE 1). Supernatant analysis may not provide accurate results of encapsulation efficiency, hence, an analogous analysis was carried out with a calibration curve to determine encapsulation efficiency involving microparticles alone. The highest EE was observed for a concentration of 5 and 10 wt% CU. For 20 wt% CU EE was significantly lower presumably due to the oversaturation phenomenon. The calculated values of drug loading reached values very close to those assumed. The slight differences observed are due to unavoidable curcumin and polymer losses at the manufacturing stage.

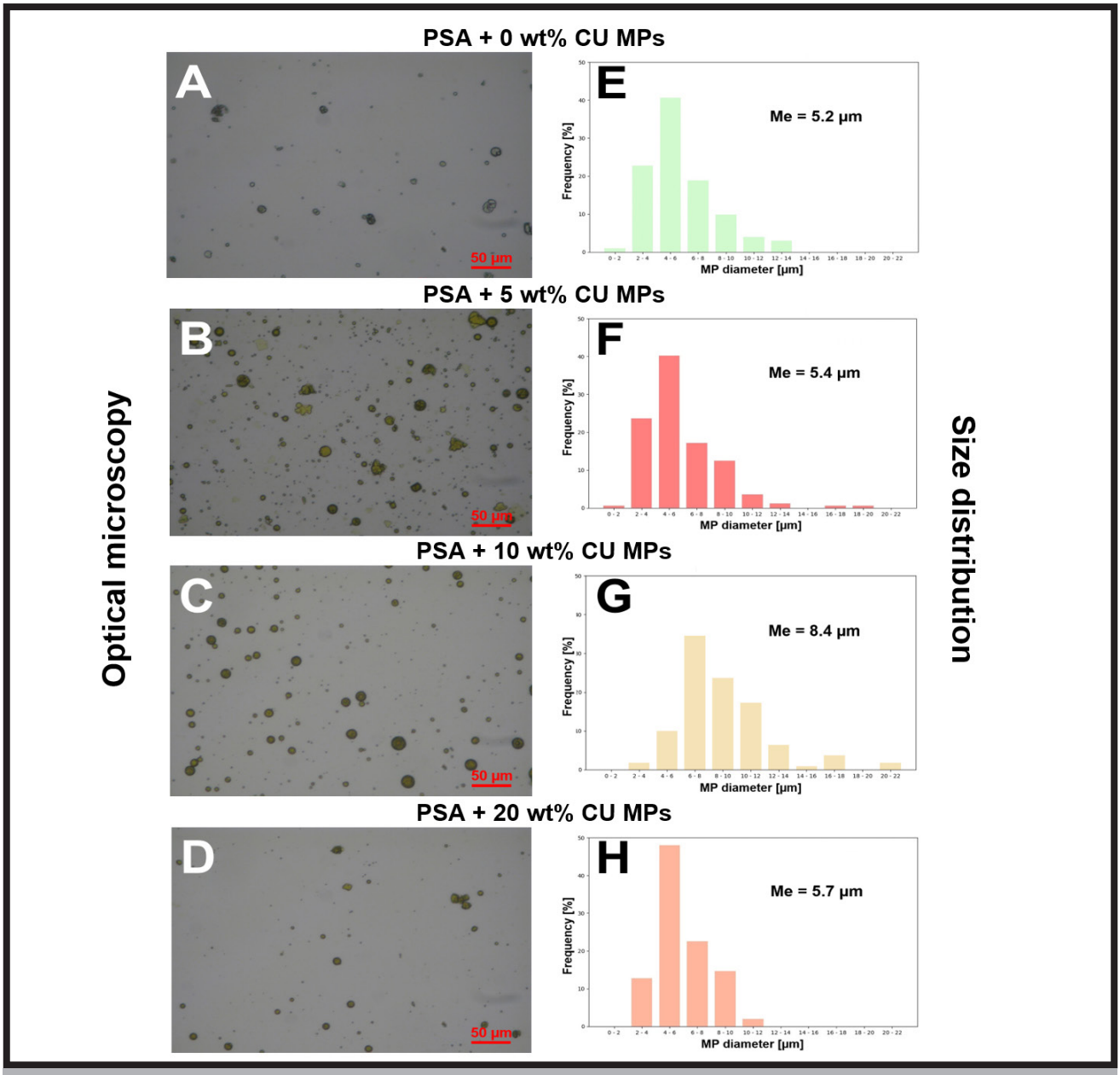

FIG. 3. Morphology (A, B, C, D) and size distribution (E, F, G, H) of PSA microparticles with different concentrations: 0 wt% CU – unloaded (A, E), 5 wt% CU (B, F), 10 wt% CU (C, G), and 20 wt% CU (D, H).

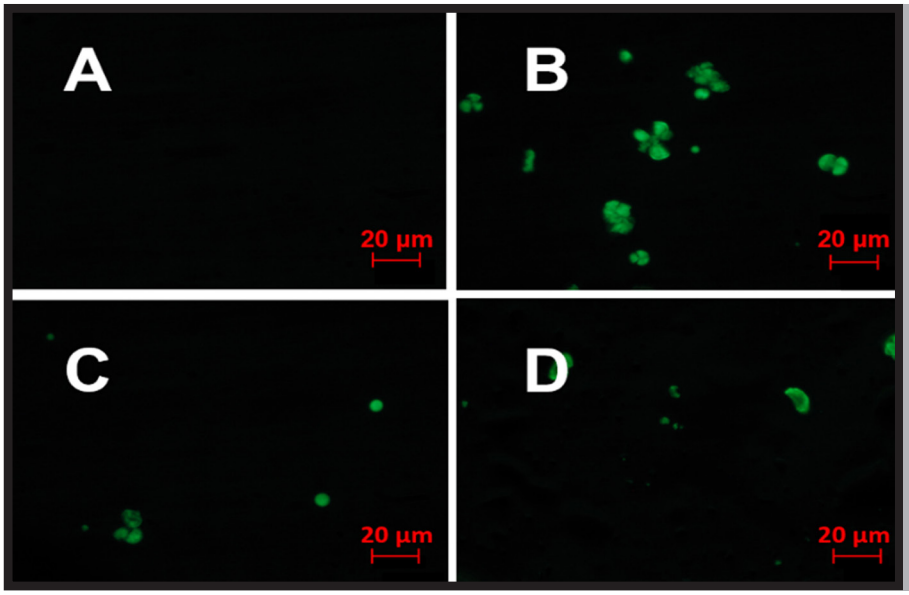

FIG. 4. Pictures from the fluorescent microscope of MPs obtained with CU: PSA with different concentrations of CU:
0 wt% CU – unloaded (A),
5 wt% CU (B),
10 wt% CU (C),
20 wt% CU (D).

TABLE 1. Curcumin encapsulation efficiency and loading in PSA+CU microparticles.

Curcumin concentration (Expected) [%]	Encapsulation efficiency EE [%]		Loading efficiency DL [%]
	supernatant analysis	microparticle analysis	-
5	81.70	72.00	5.39
10	79.50	72.50	10.53
20	58.00	52.70	17.60

FTIR analysis

The presence of CU was also determined by a semi-quantitative analysis using FTIR. FTIR analysis was performed to identify characteristic functional groups and bonds present in the curcumin molecule, confirming their successful encapsulation in the polymer carrier. Curcumin shows a characteristic band at 1510 cm^{-1}, which originates from the stretching vibrations of the C=C bonds of the aromatic ring (FIG. 5A). The spectra of the analyzed polymeric microparticle samples with encapsulated CU also show the presence of this characteristic peak at 1510 cm^{-1} (FIG. 5C-E), indicating effective encapsulation of CU in the PSA-based matrix. The intensity of this peak is highest for CU powder. For PSA samples with encapsulated CU (concentrations of 5, 10, and 20 wt% CU), the intensity of the peak changes in the same way as the encapsulation efficiency.

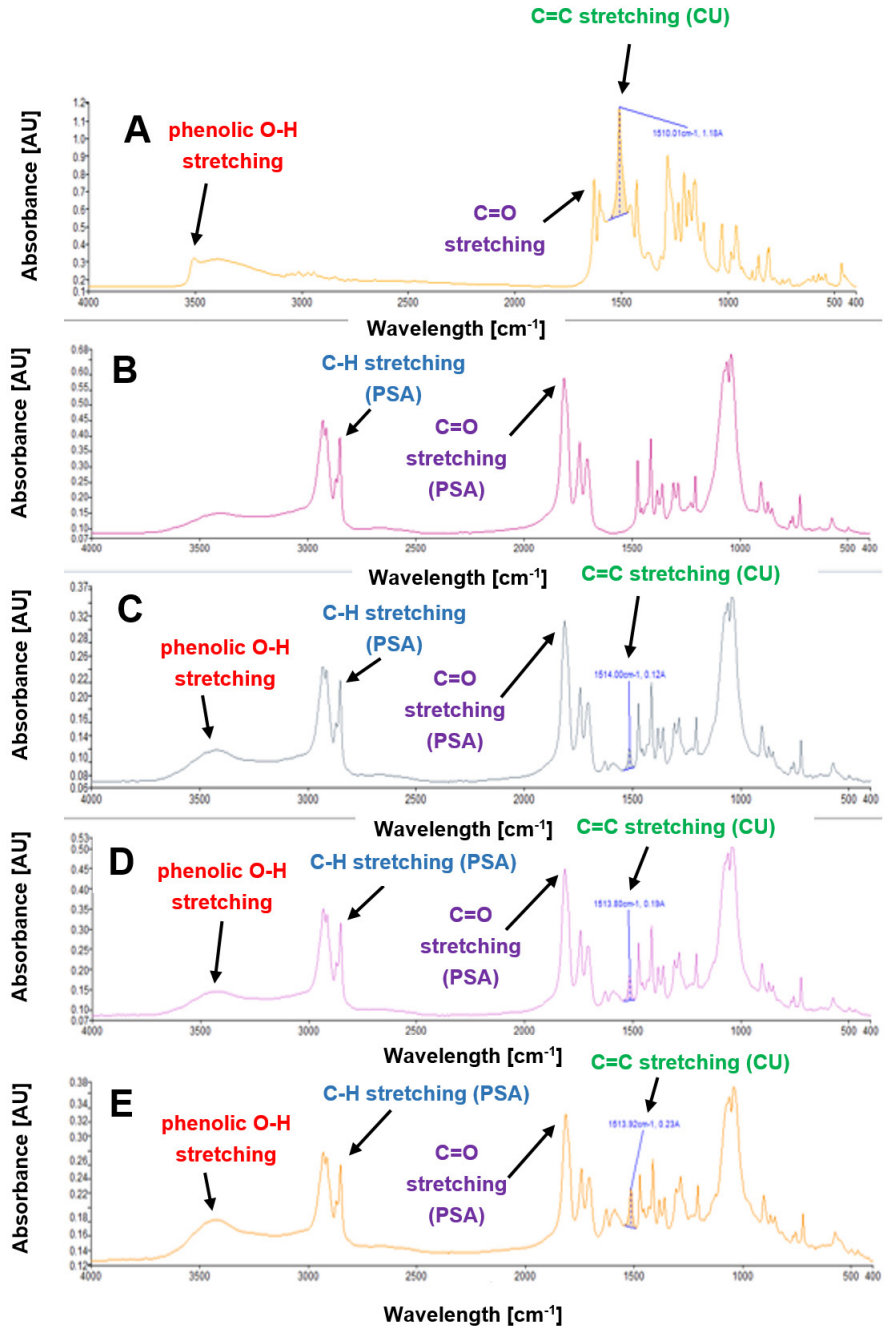

FIG. 5. FTIR spectra of the analyzed samples: CU powder (A), unloaded microparticles (B), and microparticles loaded with 5 wt% CU (C), 10 wt% CU (D), and 20 wt% CU (E).

It increases as the weight concentration of CU increases, with the peak intensity decreasing once the supersaturation value (20 wt% CU) is reached. For the unloaded microparticles sample (FIG. 5B) no peak is observed at this wavelength, indicating that CU is not present in this sample. In addition, the band from phenolic O-H stretching is present in the CU molecule (FIG. 5A) and CU-loaded samples (FIG. 5C-E) and it is absent in the PSA molecule (FIG. 5B). The characteristic functional groups for the PSA molecule (C=O carbonyl group) present at 1816 cm^{-1} and 2800 cm^{-1} (C-H stretching vibrations) were also identified and analyzed (FIG. 5B-E).

A semi-quantitative determination was carried out by analyzing the area under the curve (AUC) formed by the respective bands corresponding to the characteristic functional groups of CU and PSA. Ratios of AUC of the characteristic CU to PSA (1816 cm^{-1} to 1510 cm^{-1}) peaks may correspond to the encapsulation efficiency of CU. The ratio of PSA to PSA peaks may be an indication of the possible CU and PSA interactions. The ratio of AUC of two characteristic peaks for PSA (i.e. at 1816 cm^{-1} and 2800 cm^{-1}) was similar for all the CU-encapsulated samples, and it was higher than that for unloaded PSA microparticles; it may suggest the formation of CU-PSA bonds, probably hydrogen bonds. The ratio of AUC for the characteristic bands for CU and PSA increased for all microparticles containing CU as compared to pure CU powder. It might be proof that encapsulation was effective, but there was no direct correlation between this ratio and the expected CU loading.

In vitro studies with primary human macrophages

24 hours after macrophage activation towards M1 phenotype, microparticles of defined concentrations, together with a sample of CU powder, were dissolved in the culture medium. As a control sample, primary human macrophages alone were used. The following suspension samples of microparticles in RPMI media (concentration of CU in cell media) were tested: pure CU powder (CU at a concentration equal to 16.7 mg/mL), unloaded PSA microparticles (MPs at a concentration equal to 7.3 mg/mL), microparticles loaded with CU and tested at the concentration of 0.77 mg/mL (MPs_CU_0.77) and the concentration of 1.54 mg/mL (MPs_CU_1.54).

LDH assay

The LDH assay was performed on primary human macrophages. Cell death was assessed by the CytoTox96® assay which measures the activity of LDH released from apoptotic cells. Total LDH release was determined using LDH positive control. Cytotoxicity was defined as the percentage of LDH activity in the culture supernatants, relative to LDH activity of the positive control. The positive control was all living cells and the negative control was all dead cells. The level of control 100% (the ratio of positive to negative controls, multiplied by 100%) is equal to 54.22%. Control 100% refers to cell death. Above the line, an analyzed sample is considered cytotoxic. Three replicates for each measurement were included for each condition. The average of the three measurements was then determined. The percentage of LDH released into the culture medium was calculated as the ratio of the average to the negative control, multiplied by 100%. Based on the results, column graphs were prepared to show the % of LDH release (cell viability) for the analyzed concentrations (FIG. 6). The 100% control level was also highlighted, which marks the threshold above which the analyzed samples show a cytotoxic effect on primary human macrophages.

The results of LDH assay (FIG. 6) showed no cytotoxicity of the tested samples when cultured with primary human macrophages.

Fluorescent staining with phalloidin red and DAPI

Cell morphology was characterized using fluorescence microscopy images (Leica DMI6000 FFW, Leica Microsystems, Germany). The images were obtained at x20 magnification (FIG. 7). It was observed that when microparticles (both unloaded and curcumin-loaded) and pure CU powder were added, the cell morphology did not change. The cultured cells in contact with the added microparticles were randomly dispersed, forming numerous cell agglomerates.

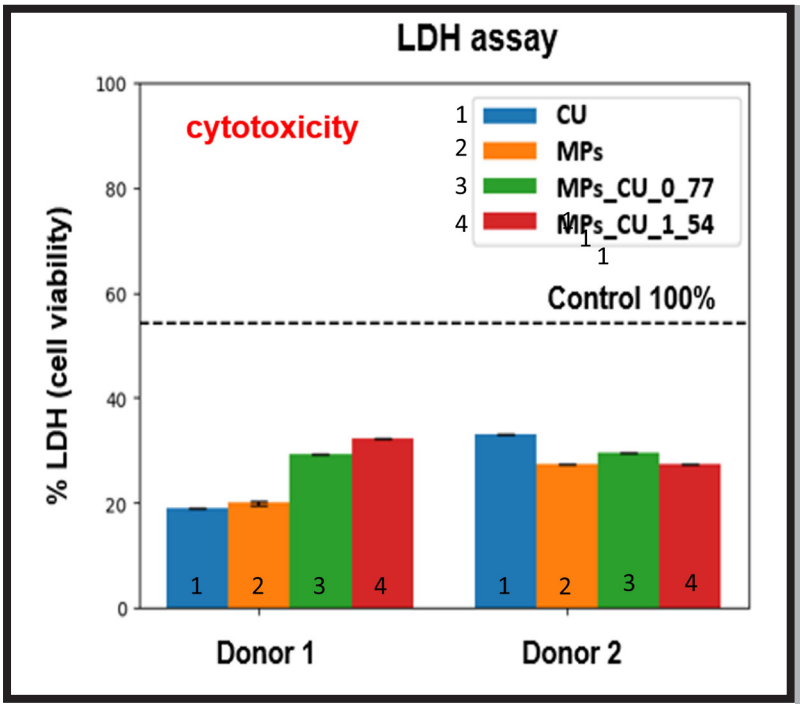

FIG. 6. Cytotoxicity assessed by the LDH assay in primary human macrophages, in contact with pure CU powder (CU), unloaded PSA microparticles (MPs), microparticles loaded with CU and tested at concentration 0.77 mg/mL (MPs_CU_0.77) and at concentration 1.54 mg/mL (MPs_CU_1.54). The 100% control represents the ratio between negative and positive controls, multiplied by 100%. n = 2.

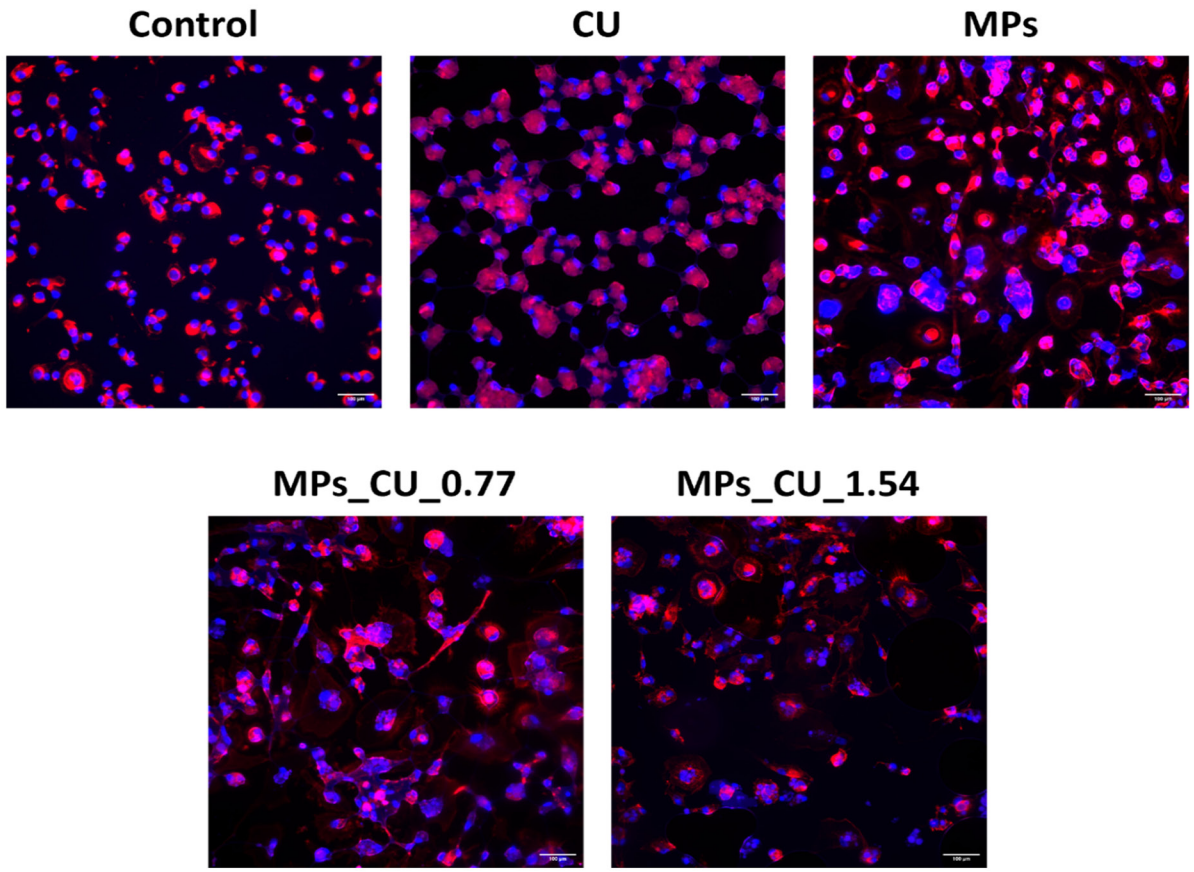

FIG. 7. Fluorescence microscopy images, at x20 objective, of human primary macrophages, derived from Donor 1, cultured in contact, for 24 h, with the following samples: control (cell culture medium), CU (curcumin powder), MPs – unloaded microparticles (PSA), and microparticles loaded with CU and tested at concentration of 0.77 mg/mL (MPs_CU_0.77) and at concentration of 1.54 mg/mL (MPs_CU_1.54).

Flow cytometry

After 24 h, the macrophages cultured with the prepared microparticles samples were collected and analyzed by flow cytometry. Dot plots from a representative experiment are presented in FIG. 8. Within each representative dot plot, a corresponding gate was determined that plotted the range of cells analyzed (TABLE 2). Gate selection (FIG. 8a-e) determines the entire cell population, which is then analyzed and assigned to phenotype M0, M1, or M2 (TABLE 2), depending on the quadrant in which the cell is located (FIG. 8A-E).

The M2/M1 ratio (number of macrophages with anti-inflammatory phenotype/number of macrophages with pro-inflammatory phenotype) is an important parameter in the context of evaluating anti-inflammatory properties. The flow cytometry analysis of macrophages was carried out for two different human donors. The results of calculating the average M2/M1 phenotypic ratio for the two donors studied (the microparticle samples analyzed were CU, MPs, MPs_CU_0.77, and MPs_CU_1.54) are shown in TABLE 2. The results obtained indicate that the presence of CU increases the M2/M1 phenotypic ratio, promoting macrophage polarization towards the M2 (anti-inflammatory) phenotype.

Based on the data collected in TABLE 2, the values of the M2/M1 phenotypic ratios for the two different donors are presented graphically in FIG. 9 as Average ± standard deviation of the sample (SD). The results show that the addition of CU or CU-loaded microparticles to the cell culture media results in an increased M2/M1 ratio.

The M2/M1 ratio for the samples with CU and CU powder is significantly higher than for the samples unloaded with CU. At the same time, the flow cytometry results indicated the presence of only a few anti-inflammatory cells, which may suggest that PSA-based microparticles with encapsulated curcumin at the concentrations tested in this research do not exhibit sufficient anti-inflammatory properties to reduce inflammation at the wound site. Therefore, it would be interesting for future studies to test earlier time points (for example, less than 24 h). To obtain more reliable results, it would be necessary to increase the number of donors.

Ethics statement

Human primary monocytes were isolated from surplus buffy coats from healthy blood donors, kindly donated by Serviço de Imunohemoterapia, Centro Hospitalar Universitário de São João (CHUSJ), Porto. All obtained human samples and procedures were performed in agreement with the principles of the Declaration of Helsinki and all experimental protocols were conducted following the approval and recommendations of the CHUSJ Ethics Committee for Health (references 90/19 and 260/11). Written informed consent was obtained from all subjects before sample collection. Buffy coat samples were provided anonymized and patient identification was not provided to researchers.

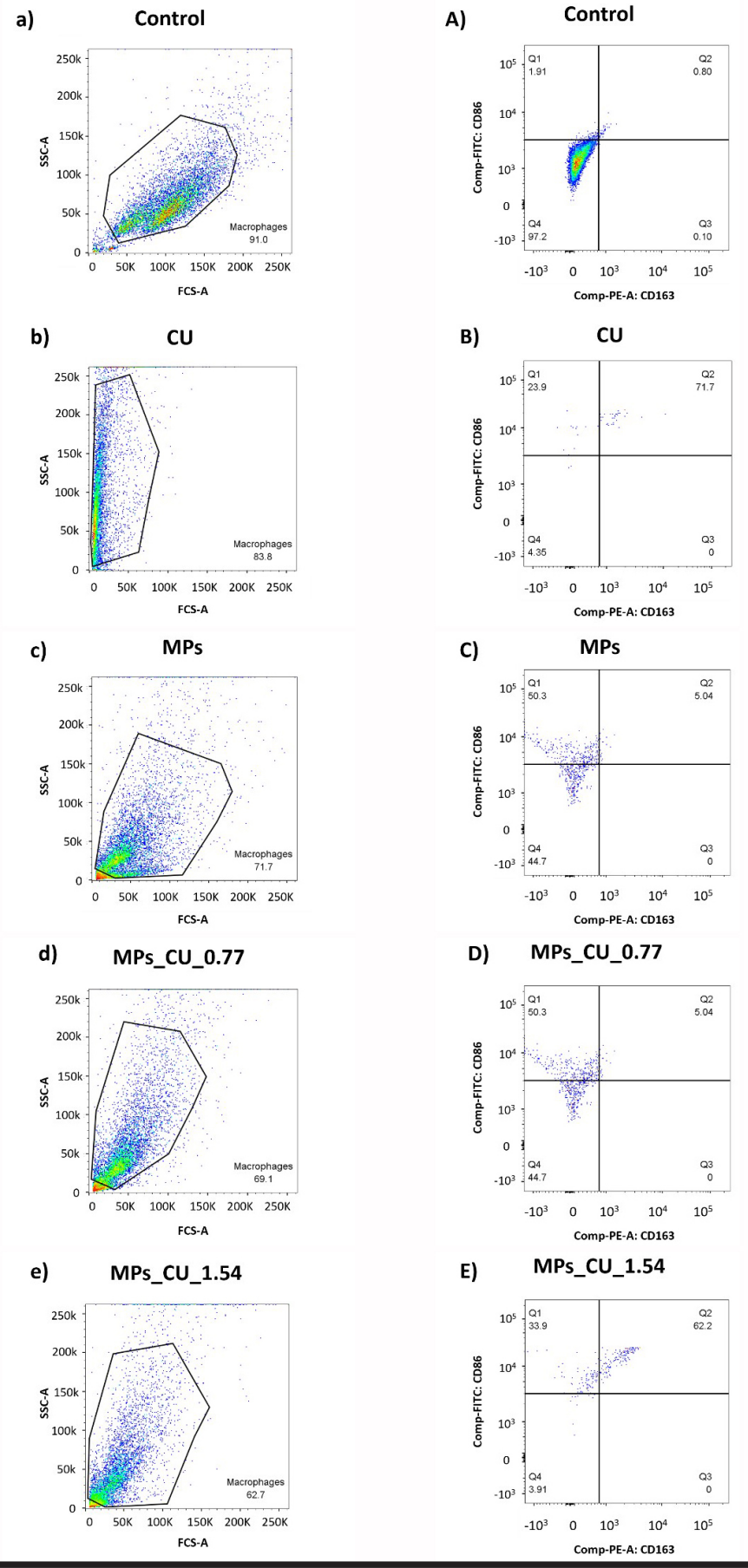

FIG. 8. Expression of cell surface markers on macrophages. Representative dot plots showing: a)-e) aspect ratio; A)-E) expression of CD14, CD86, and CD163 antigens. Gates were drawn from isotype control staining. Percentage of CD14 positive cells expressing CD163 (M2 marker) and/or CD86 (M1 marker) antigens (FSC: forward scatter; SSC: side scatter).

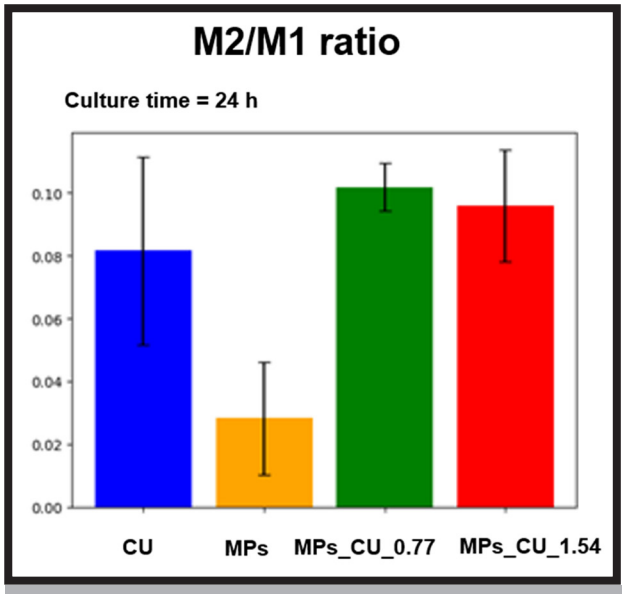

FIG. 9. Characterization of the averaged ratio M2 to M1 macrophages from two donors as studied by flow cytometry in contact with the following samples: CU, MPs, MPs_CU_0.77, and MPs_CU_1.54.

Conclusions

In this study, PSA microparticles loaded with CU were developed as a component of dressing for the treatment of ulcers occurring in diabetic foot syndrome. The carriers were spherical and of the 5-8 μm median size, thus suitable to be suspended in topical formulations administered to wounded skin [14]. Encapsulation efficiency of 72% was achieved for the sample with 10 wt% CU microparticles. The presence of CU in microparticles was also confirmed by:
1) visual inspection (yellow colour contrarily to white colour for unloaded microparticles, FIG. 3);
2) fluorescent properties (polymer matrix does not exhibit fluorescence but curcumin molecule does, FIG. 4);
3) presence of bands in FTIR spectra characteristic for pure curcumin (FIG. 5).

CU carriers were tested for cytotoxicity in contact with primary human macrophages. Their phenotype (M1-pro-inflammatory, M2-anti-inflammatory) and M2/M1 ratio were determined by flow cytometry analysis. The LDH tests showed that the obtained microparticles are not cytotoxic and that the phenotypic M2/M1 ratio for samples with CU and CU powder is higher than for samples without CU. This confirms that curcumin released from the microparticles is able to increase the polarization of macrophages toward an anti-inflammatory phenotype, what may be explored in the development of dressings for the treatment of diabetic foot ulcers.

TABLE 2. Flow cytometry analysis of studied macrophages (number of cells) from two different donors shown as average and SD.

Sample	CD14	CD86 (M1)	CD163 (M2)	Ratio M2/M1 Average ± SD
CU	1659	17355	1424	0.082 ± 0.029
MPs	2017	4081	114	0.028 ± 0.082
MPs_CU_0.77	1955	10451	1064	0.102 ± 0.007
MPs_CU_1.54	1662	13106	1256	0.096 ± 0.018
Culture time = 24 h				

Acknowledgements

The research was supported by the subsidy (No 16.16.160.557) for the AGH University of Krakow, and the Norte Regional Operational Program, Portugal – Structured R&D&I Projects – Unorte.pt. HEALTH-UNORTE;NORTE-01-0145-FEDER 000039 for i3s Institute, Porto. KW is acknowledging Erasmus Plus program for the support of her stay at i3S – Instituto de Investigação e Inovação em Saúde, Universidade do Porto. The authors thank Prof. Katarzyna Jaszcz from Silesia University of Technology for providing poly(sebacic anhydride) samples.

ORCID iD

K. Wójcik: https://orcid.org/0009-0005-0944-0234
A. Kusibab: https://orcid.org/0000-0002-5580-7392
A.B. Sousa: https://orcid.org/0000-0002-3460-0499
J. Novais Barbosa: https://orcid.org/0000-0003-1852-2790
E. Pamuła: https://orcid.org/0000-0002-0464-6189

References

[1] Kandregula B., Narisepalli S., Chitkara D.: Exploration of Lipid-Based Nanocarriers as Drug Delivery Systems in Diabetic Foot Ulcer. Molecular Pharmaceutics 19(7) (2022) 1977–1998, doi:10.1021/acs.molpharmaceut.1c00970.
[2] Gowthamarajan K., Karri V.V.S.R., Satish Kumar M.N.: Multiple Biological Actions of Curcumin in the Management of Diabetic Foot Ulcer Complications: A Systematic Review. Tropical Medicine and Surgery 3 (2015) 179, doi:10.4172/2329-9088.1000179.
[3] Akhtar S., Latif M., Ahmed O.S., Sarwar A., Alina A., Khan M.I.: Prevalence of foot ulcers in diabetic patients in Punjab, Pakistan. Fronteries in Public Health 8(10) (2022) 967733, doi:10.3389/fpubh.2022.967733.
[4] Salad A.M., Duale H.A., Sheikh I.M., Hassan G.D., Farah A.A., Gele A.: Prevalence of diabetes foot ulcers and associated factors among adult diabetic patients in three referral hospitals in Mogadishu, Somalia. Fronteries in Public Health 11 (2023) 1195483, doi:10.3389/fpubh.2023.1195483.
[5] Driver V.R., Fabbi M., Lavery L.A., Gibbons G.: The costs of diabetic foot: The economic case for the limb salvage team. Journal of Vascular Surgery 52(3) (2010) 17S-22S, doi:10.1016/j.jvs.2010.06.003.
[6] Spampinato S.F., Caruso G.I., De Pasquale R., Sortino M.A., Merlo S.: The Treatment of Impaired Wound Healing in Diabetes: Looking among Old Drugs. Pharmaceuticals 13(4) (2020) 60, doi:10.3390/ph13040060.
[7] Akbik D., Ghadiri M., Chrzanowski W., Rohanizadeh R.: Curcumin as a wound healing agent. Life Sciences 116(1) (2014) 1–7, doi:10.1016/j.lfs.2014.08.016.
[8] Krzyszczyk P., Schloss R., Palmer A., Berthiaume F.: The Role of Macrophages in Acute and Chronic Wound Healing and Interventions to Promote Pro-wound Healing Phenotypes. Fronteries in Physiology 9 (2018) 419, doi:10.3389/fphys.2018.00419.
[9] Sousa A.B., Águas A.P., Barbosa M.A., Barbosa J.N.: Immunomodulatory biomaterial-based wound dressings advance the healing of chronic wounds via regulating macrophage behaviour. Regenerative Biomaterials 9 (2022) rbac065, doi:10.1093/rb/rbac065.
[10] Jaszcz K.: Synthesis and Characterization of New Functional Poly(ester-anhydride)s Based on Succinic and Sebacic Acids. Macromolecular Symposia 254(1) (2007) 109–116, doi:10.1002/masy.200750817.
[11] Kwiecień K., Reczyńska-Kolman K., Niewolik D., Jaszcz K., Pamuła E.: Poly(sebacic anhydride) microparticles loaded with curcumin for pulmonary purposes. Engineering of Biomaterials 162(24) (2021), doi:10.34821/eng.biomat.162.2021.7-12.
[12] Oliveira M.I., Pinto M.L., Gonçalves R.M., Martins M.C.L., Santos S.G., Barbosa M.A.: Adsorbed Fibrinogen stimulates TLR-4 on monocytes and induces BMP-2 expression. Acta Biomaterialia 49 (2017) 296–305, doi:10.1016/j.actbio.2016.11.034.
[13] Bessa-Gonçalves M., Silva A.M., Brás J.P., Helmholz H., Luthringer-Feyerabend B.J.C., Willumeit-Römer R., Barbosa M.A., Santos S.G.: Fibrinogen and magnesium combination biomaterials modulate macrophage phenotype, NF-kB signaling and crosstalk with mesenchymal stem/stromal cells. Acta Biomaterialia 114 (2020) 471–484, doi:10.1016/j.actbio.2020.07.028.
[14] Reczyńska-Kolman K., Hartman K., Kwiecień K., Brzychczy-Włoch M., Pamuła E.: Composites Based on Gellan Gum, Alginate and Nisin-Enriched Lipid Nanoparticles for the Treatment of Infected Wounds. International Journal of Molecular Sciences 23(1) (2022) 321, doi:10.3390/ijms23010321.